
A New Lightweight Porous Structures for Reusable Energy Absorption in Heavy-loaded Planetary Landers

Chengbo CUI^a, Jianguo CAI^{*a}, Meng LI^{*b}

^{*a}Key Laboratory of C & PC Structures of Ministry of Education, National Prestress Engineering Research Center, Southeast University, Nanjing 211189, China

j.cai@seu.edu.cn

^{*b}Qian Xuesen Laboratory of Space Technology, China Academy of Space Technology, Youyi Street No. 104, Haidian, Beijing 100094, China
limeng_qianlab@163.com

Abstract

In future planetary surface exploration missions, to expand the exploration area, more and more landers will perform multiple long-range landings in a single mission. With the development of aerospace technology, the weight of landers is showing an increasing trend. This has sparked a demand for lightweight, heavy-loaded, and reusable energy-absorbing structures. Our research presents a novel porous structure with high energy absorption, achieved by integrating origami and shape memory alloys into honeycomb designs. The use of Ni-Ti alloys allows for recovery from non-elastic deformation, while origami techniques enhance structural integrity under heavy loads. To address the difficulty in describing the deformation behavior of the new porous structure during multiple compression cycles, a parametric surrogate model for reusable energy-absorbing performance was developed using machine learning techniques. Experimental and finite element verification showed that the reusable energy-absorbing capability of the new porous structure is more than 8 times that of traditional honeycomb structures, can withstand more than 10 loading-unloading cycles, and has an energy-absorbing capability decay of less than 10%. These findings indicate that our design is well-suited to meet the stringent requirements for reusable energy-absorbing capabilities in future space mission equipment.

Keywords: Planetary Landers, Reusable energy-absorbing Structures, Shape Memory Alloy; Miura Origami, Machine learning

1. Introduction

As the Artemis program by the United States National Aeronautics and Space Administration (NASA) and China's International Lunar Research Station (ILRS), alongside other lunar exploration initiatives. The demand for extensive lunar surface exploration, exploration of the lunar polar regions, and the establishment of lunar bases is increasing. These missions necessitate not only successful landings on the surface of deep-space planets but also a diverse range of exploration capabilities, the ability to transport a significant number of personnel and goods, and swift responses to emergencies[1-3]. Currently, lunar rovers represent the most advanced extraterrestrial mobile vehicles. However, due to constraints in launch mass, even the most extensively traveled lunar rover in history, Lunokhod 2, has covered only 37 kilometers. Moreover, the unique properties of lunar soil could render a lunar rover immobile if it moves too fast or carries an excessively heavy load[4-8].

In light of these challenges, planetary landers equipped for multiple launches and landings offer significant advantages. They possess the capacity to carry substantial payloads, robust obstacle-

crossing capabilities, rapid responsiveness, and the potential for reuse. Consequently, they emerge as the optimal choice for future planet surface vehicles.

1.1. Planetary Landers

In the numerous planetary surface exploration endeavors undertaken by humanity, there have been 25 successful soft landings on the Moon and 17 on the Martian surface. Among these, the three predominant landing buffer methods are leg landing buffer, airbag landing buffer, and sky crane [9-11]. The leg landing buffer is the most frequently employed method for planetary landers, utilizing a buffer structure situated between the inner and outer cavities of the landing leg to absorb impact energy. This method outperforms the airbag buffers and sky crane in terms of landing stability, adjustability of landing attitude, and lower requirements for atmospheric conditions during landing. The multi-block aluminum honeycomb structure is commonly implemented as the buffer structure in leg landing mechanisms. Its plastic deformation allows for the absorption of impact energy during landing. Owing to the vacuum of space and extreme temperature fluctuations, the use of an aluminum honeycomb structure as a buffer mitigates issues associated with liquid sealing and temperature control that arise when using compressible liquids as buffer structures [12].

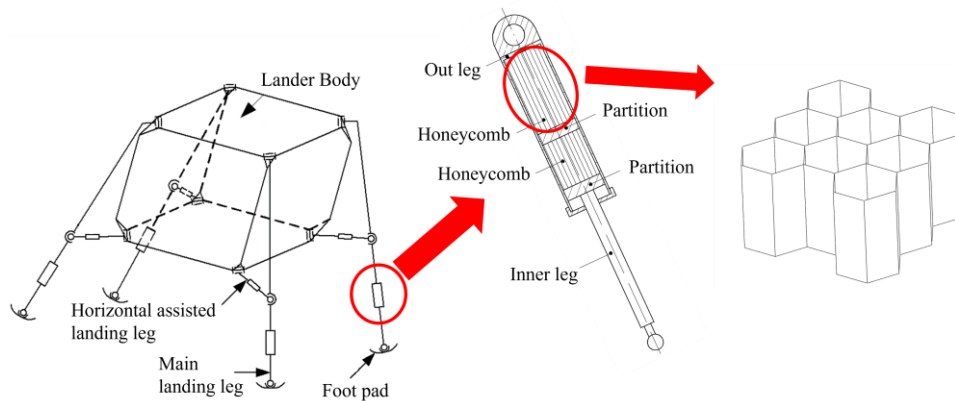


Figure 1: Structural diagram of typical legged lander. The landing leg of the legged lander is composed of the main landing leg, the horizontal assisted landing leg and the foot pad. The main landing leg and the horizontal assisted landing leg absorb the impact kinetic energy in the vertical and horizontal directions respectively. The honeycomb structure is installed between the outer leg and the inner leg of the landing leg as a buffer energy absorption structure[9-11].

1.2. Honeycomb Structures

For legged landers equipped with multi-block honeycomb structures as energy absorbers, the cushioning performance is predominantly dictated by the behavior of the metallic honeycomb within the landing legs. Consequently, investigating the mechanical properties of honeycomb structures, particularly in terms of platform stress and specific energy absorption, is crucial for enhancing the lander's cushioning design [13-16]. McFarland [17] pioneered a theoretical model to assess the Z-directional cushioning performance of metal honeycombs. This was later refined by Chen and Wierzbicki [25], who introduced the simplified superfold element method, establishing a direct correlation between honeycomb parameters and mechanical attributes, rendering theoretical analysis of cushioning performance both intuitive and efficient.

To augment the energy absorption capabilities of honeycomb structures, recent studies have focused on modifying their design through varied topological configurations such as triangular [18,19], I-shaped [20], square [19,21], and circular [22,23] patterns. Findings indicate that honeycombs with analogous topologies exhibit minor differences in energy absorption characteristics, with an observed increase in buffer performance relative to density. Additionally, innovative topological designs like hierarchical [24], negative Poisson's ratio [25], and arrow-shaped [25] honeycomb structures have been integrated into design schemes. Notably, the hierarchical honeycomb structure has demonstrated

an in-plane mass-specific energy absorption approximately 2.5 times greater than conventional honeycomb structures [24]. The negative Poisson's ratio and arrow-shaped honeycomb structures exhibit secondary strengthened stress levels upon compression, offering significant potential for seismic design applications [25].

The incorporation of novel topological cells substantiates the potential for altering cellular deformation and mechanical properties through modifications to cellular topological structures.

1.3. Shape Memory Alloy Porous Structures

The NiTi shape memory alloy is a type of phase change material characterized by its phase transitions between different crystal configurations, which endows it with notable recoverable inelastic deformation properties. In related research endeavors, the NiTi alloy has been implemented within porous structures, such as those mimicking a honeycomb, capitalizing on its capacity for resilient inelastic deformation. This application not only upholds structural rigidity but also confers upon the structure the capability for repeated impact buffering and energy absorption.

Shaw et al. [26] fabricated a reusable honeycomb structure utilizing superelastic NiTi alloy, employing niobium-based brazing techniques, and subjected it to multiple coplanar compression cycles. The experimental outcomes indicated that the NiTi alloy honeycomb possesses a consistent hysteretic energy consumption capacity, which remains stable post the second loading and unloading cycle. However, an incremental increase in structural strain was observed to induce residual strains surpassing the phase transformation strain of the NiTi alloy upon structural unloading. This investigation preliminarily substantiated the potential application of NiTi alloy-based honeycomb structures for reusable energy absorption in impact buffering [27]. Additional explorations have been conducted to extend the use of shape memory alloys to innovative topological porous structures, including circular tubes [28,29], lattice structures [30], and wire truss configurations [31]. These comprehensive studies have affirmed the highly reusable buffering capabilities of shape memory alloy porous structures. With judicious design, limiting the degree of local structural deformation results in minimal degradation of the structure's reusable buffer performance and residual deformation upon unloading. Despite these advancements, the special processing requirements associated with NiTi alloy have historically restricted the scope of research on its application in reusable energy-absorbing porous systems. Current research primarily focuses on proof-of-concept experiments, and although the reusability of buffer performance has been corroborated, there remains a paucity of targeted design methodologies aimed at mitigating local deformation through structural optimization [27].

In this paper, we propose an origami honeycomb structure composed of NiTi shape memory alloy, for the demanding, reusable energy absorption requirements encountered during multiple launch and landing operations of planetary landers. First, the recoverable inelastic deformation characteristics of the NiTi shape memory alloy were investigated via simulation and experimentation. Second, the geometric features of the origami honeycomb and their influence on the mechanical performance of the honeycomb structure were analyzed. Finally, by mathematically describing the conditions of planetary descent, an optimization model for the energy absorption performance of the origami honeycomb structure was formulated. The design of a new porous structure was intended for heavy-loaded applications in planetary lander technology.

2. Reusable Energy Absorption Porous Structure

2.1. Honeycomb with Origami

As shown in Figure 2 (a), when the honeycomb structure used for the legged landing buffer is plastic deformed under impact in Z direction, the cell will be folded and deformed. At the crease caused by cell folding, the plastic hinge absorbs energy through inelastic bending deformation to realize the buffering and energy absorption of the honeycomb structure. The folded cells generated by the honeycomb structure under compression in the out of plane direction show a periodic arrangement, and have a topology similar to that of Miura origami cells. By adding Miura creases to the traditional hexagonal honeycomb structure, a new origami honeycomb structure is formed.

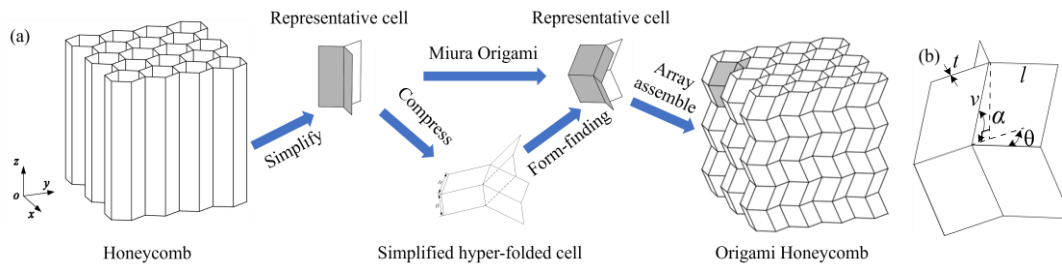


Figure 2: (a) Form finding process of origami honeycomb structure. When the honeycomb structure is compressed in the Z direction, the cells will be folded, and the crease position will be plastically deformed to achieve energy absorption. The cell of the honeycomb structure is combined with the Miura origami unit to obtain the origami honeycomb structure. After that, the origami honeycomb structure is arrayed to obtain the origami honeycomb structure. (b) Schematic diagram of the cell of origami honeycomb structure. The geometric design parameters of origami honeycomb structure include unit height H , cell wall length l , cell wall thickness t , inclined side length v , in-plane angle α and line surface angle θ

The structural characteristic parameters of the origami honeycomb structure include the unit height H , cell wall length l , cell wall thickness t , inclined side length v , and in-plane angle α , as well as the line surface angle θ . Upon impact and deformation in the Z direction, the honeycomb structure undergoes plastic deformation, which initiates preferentially at the crease position. This leads to a specific mode of plastic deformation for the honeycomb structure, expanding the area involved in plastic deformation and reducing the degree of local plastic deformation. This phenomenon facilitates the realization of a reusable energy-absorbing porous structure through the reusable inelastic deformation of shape memory alloys.

2.2. NiTi Shape memory alloy

The NiTi shape memory alloy is a kind of phase change material capable of recovering a certain degree of inelastic deformation through the transformation of various crystal phases. This occurs when the service temperature exceeds the end temperature of austenite transformation (A_f) and falls below the critical temperature for stress-induced martensitic transformation (M_d). Subsequently, the material enters a plastic deformation region due to stress-induced austenite martensitic transformation following elastic deformation. This phenomenon is referred to as the hyper-elastic or pseudo elastic effect, as the plastic deformation region can be restored through a crystal phase transition similar to elastic deformation upon unloading.

The experimental measurement of the reusable inelastic deformation properties was conducted on a shape memory alloy with a NiTi atomic ratio of 51:49, which exhibited room temperature hyper-elasticity. The alloy underwent processes including ingot casting, cutting, wire drawing, and annealing at 400°C for 3 minutes. Subsequently, an 80mm length of the NiTi alloy wire was obtained. The WDT II-10 universal tensile testing machine was employed to perform the tensile loading-unloading cycle, applying an overall strain of 8% at 30°C. Force-displacement data throughout the test were meticulously recorded.

ABAQUS, a finite element simulation software, employs a macroscopic phenomenological model based on Auricchio to calculate the volume fraction of martensite, denoted as ξ . The hyper-elastic effect material model for shape memory alloys is conceptualized with an internal variable approach. This model was utilized in ABAQUS to simulate the tensile loading and unloading process of shape memory alloy wire, and the resulting stress-strain curves from both experimental tests and simulations were comparatively analyzed. It is evident that with appropriate material parameters, NiTi alloy wire exhibits consistent mechanical behavior between the tensile test and simulation, indicating a minimal discrepancy in mechanical properties, which attests to the model's reliability.

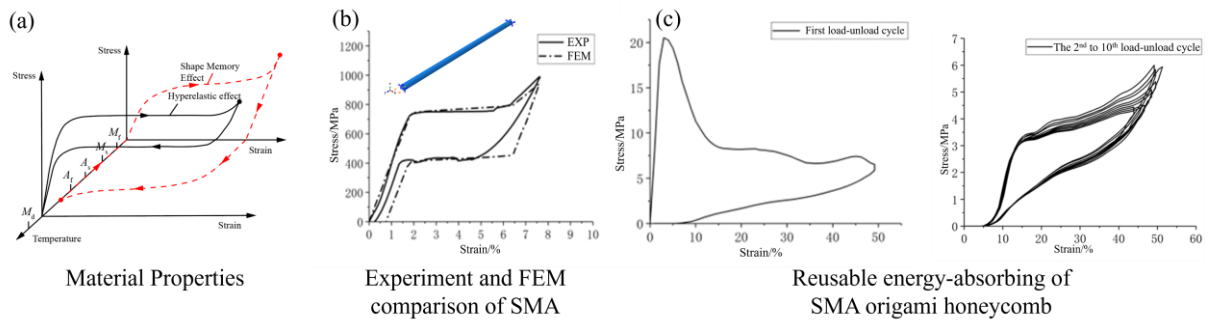


Figure 3: (a) Mechanical properties of shape memory effect and hyper-elastic effect of NiTi shape memory alloy at different temperatures. (b) The experiment and FEM tensile load-unload cycle stress-strain curve of NiTi shape memory alloy wire was compared. (c) Reusable energy absorption performance of shape memory alloy origami honeycomb structure.

The shape memory alloy origami honeycomb simulation model was constructed, and displacement compression was applied along the Z direction. The loading and unloading cycle were executed 10 times, during which the stress-strain behavior of the honeycomb structure was documented. Analysis of the stress-strain curve reveals several key observations. First, it is evident that the shape memory alloy origami honeycomb structure exhibits a distinct energy dissipation hysteresis loop during cyclic compression, signifying its capacity for reusable energy absorption. Second, the curve demonstrates a pronounced energy absorption plateau within the reusable buffer section, indicating that this energy absorption performance is attributable to the recoverable inelastic deformation of the material. Finally, the reusable buffer energy absorption performance of the origami honeycomb structure stabilizes after the third loading cycle; however, there is a slight diminishment in the energy dissipation capacity with an increase in loading cycles due to material degradation.

3. Design for the Heavy-loaded Planet Landers

3.1. Landing Conditions

The deployment of a planetary lander onto the surface of a distant celestial body is an intricate process involving motion control and coupling. To more accurately articulate the future requirements for reusable energy-absorbing devices in planetary landers, an analysis was conducted on the operational conditions of the reusable honeycomb structure based on the current planetary lander design. This analysis was then translated into a mathematical representation.

In the context of the quadra-legs lander, there exist three primary landing modes: (1) The full landing mode, wherein all four landing legs make contact with the planet's surface simultaneously; (2) The “2-2” landing mode, characterized by an initial contact with two landing legs followed by the subsequent engagement of the remaining two legs; and (3) The “1-2-1” landing mode, which commences with a single landing leg touching down, followed by two adjacent legs, and culminates with the landing leg in the diagonal position.

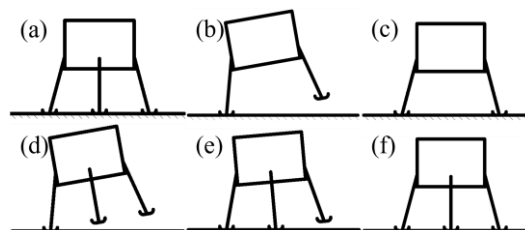


Figure 4: (a) Full landing mode; (b) and (c) “2-2” Landing mode; (d)-(f) “1-2-1” Landing mode.

For a given landing condition, the lower bound of the honeycomb buffer's capacity is dictated by the potential and kinetic energy of the lander at the moment of impact. Conversely, the upper bound is defined by the maximum permissible acceleration experienced by the protected object, which is a

consequence of the reaction force exerted during the landing process. Thus, the landing dynamics of the planetary surface lander can be encapsulated in the following expression:

$$\overline{\sigma}_r A_{\text{Total}} L_E = M \left(\frac{1}{2} v_{\text{impact}}^2 + g_{\text{Local}} H \right) \quad (1)$$

$$\overline{\sigma}_r A_{\text{Total}} \cos \phi \leq M[a] \quad (2)$$

$$\text{Opt.} \begin{cases} \text{Max: } SEA_m \\ \text{s.t: } \overline{\sigma}_r \leq [\sigma_s] \\ W \geq E \\ \omega_1 \leq \omega \leq \omega_2 \end{cases} \quad (3)$$

$\overline{\sigma}_r$ is the platform stress of the reusable inelastic deformation process of the buffer structure; A_{Total} is the vertical cross-sectional area of the buffer structure for deformation energy absorption; L_E is the reusable energy absorption length of the buffer structure; M is the mass of the lander; v_{impact} is the landing speed of the lander; g_{Local} is the gravitational acceleration of the planet surface; H is the height change of the center of mass of the lander during landing. $[a]$ is the maximum allowable acceleration of the lander load; ϕ is the normal angle between landing leg and planet surface. SEA_m is mass specific energy absorption; $[\sigma_s]$ is the maximum allowable platform stress calculated from the maximum allowable acceleration; ω is the parameter vector of origami honeycomb structure; ω_1 and ω_2 represent the parameter vectors of the lower and upper bounds of the origami honeycomb structure parameters respectively.

3.2. Structure Optimization

Referencing the parameters of NASA's Apollo series lunar landing spacecraft, we have formulated the optimization design problem as demonstrated. Leveraging the validated finite element simulation model and machine learning techniques, we have constructed a numerical surrogate model for the reusable buffer performance of the SMA origami honeycomb structure. This surrogate model is integrated into the optimization design process to derive the parameters for the reusable energy-absorbing honeycomb structure that fulfills the operational requirements of the planetary lander. The reusable buffer performance of the optimized origami honeycomb structure is subsequently substantiated through finite element simulation.

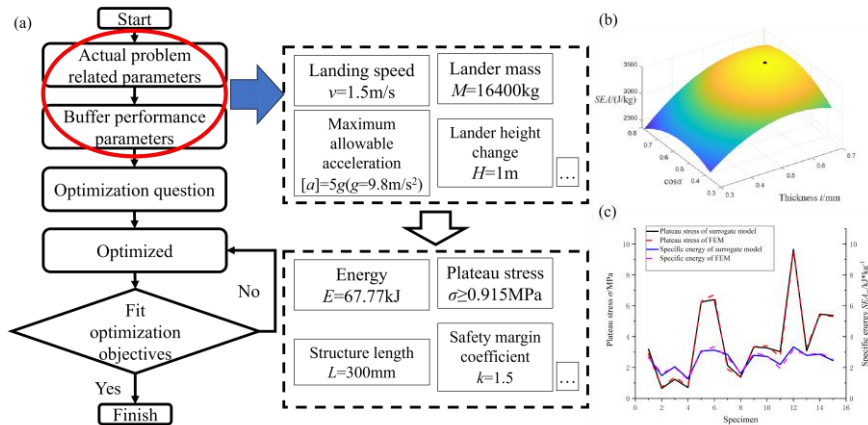


Figure 5: (a) Optimized design flow chart; (b) The design surface of the surrogate model; (c) The comparison of surrogate model and FEM among specimens.

4. Conclusion

In this study, a shape memory alloy honeycomb structure is introduced for future planetary landers designed to withstand heavy loads and multiple launch-landing cycles. The integration of origami principles into the honeycomb structure enhances its ability to deform and absorb energy during compression, thereby increasing the energy absorption area, minimizing local deformation, and enabling reusable cushioning for energy absorption. A mathematical surrogate model for reusable cushioning performance is developed based on a finite element simulation validated by experimental results. The landing conditions for the planetary lander are translated into a mathematical model, and an optimization design process for the SMA cellular structure's reusable cushioning performance is formulated. The reliability of this optimization design process is confirmed through the execution of an exemplary optimization design.

Acknowledgements

This research was funded by the National Natural Science Foundation of China, grant number 52275279.

References

- [1] Y. J. Tian, M. Zhang, Q. Lin, "Functional requirements analysis and research status of large-scale lunar surface detection," *Manned Spaceflight*, vol. 26, no. 5, pp. 649-655, 2020.
- [2] T. S. Zhang, "Water found on the illuminated surface of the moon," *Aerospace China*, vol. 2020, no. 12, pp. 80-81, 2020.
- [3] D. Y. Yu, J. N. Ma, "Progress and Prospect of deep space exploration in China," *Science and Technology Foresight*, vol.1, no. 1, pp. 17-27, 2022.
- [4] Y. X. Chen, "Design of self unloading lunar rover and lunar landing spacecraft," *National Defense Technology*, vol. 1, pp. 1-130, 1996.
- [5] R. X. Zhan, S. M. Li, W. Y. Shang, "Obstacle avoidance behavior of Lunar Rover Based on fuzzy pattern recognition," *Computing Technology and Automation*, vol. 1, pp. 6-8, 2008.
- [6] Z. Q. Deng, "Technical research and development of lunar rover," *Proceedings of the 2002 annual meeting of Heilongjiang Mechanical Engineering Society*, 2002.
- [7] L. Y. Deng, J. F. Guo, N. G. Cui, "Research progress and Prospect of lunar base engineering," *Missiles and Space Vehicles*, vol. 2, pp. 25-30, 2009.
- [8] X. L. Ding, X. Y. Shi, A. ROVETTA, "Development and Prospect of lunar rover robot technology," *Robot Technology and Application*, vol. 3, pp. 5-9, 2008.
- [9] C. J. Luo, "Theoretical model and optimal design of legged landing buffer," *Harbin Institute of Technology*, 2010.
- [10] C. Wang, "Design of four leg truss lunar landing device and Research on landing buffer technology," *Harbin Institute of Technology*, 2008.
- [11] M. Li, R. Q. Liu, H. W. Guo, "Optimization design of energy absorption characteristics of metal honeycomb with different topological structures for legged Lander," *Journal of Vibration and Shock*, vol. 32, no. 21, pp. 7-14, 2013.
- [12] H. S. Han, Y. R. Wang, Y. P. Jiang, "Characteristics and application of landing buffer system for foreign deep space probe," *Spacecraft Engineering*, vol. 21, no. 6, pp. 7-24, 2012.
- [13] K. Li, X. L. Gao, J. Wang, "Dynamic crushing behavior of honeycomb structures with irregular cell shapes and non-uniform cell wall thickness," *International Journal of Solids & Structures*, vol. 44, no. 14-15, pp. 5003-26, 2007.
- [14] J. L. Yu, Z. J. Zheng, "Dynamic crushing of 2D cellular metals: Microstructure effects and rate-sensitivity mechanisms," *Acta Mech Solida Sin*, vol. 23, no. S, pp. 45-55, 2010.

- [15] H. Yin, G. Hou, "Crushing analysis and multiobjective crashworthiness optimization of honeycomb-filled single and bitubular polygonal tubes," *Materials & Design*, vol. 32, no. 8, pp. 4449-4460, 2011.
- [16] M. Yamashita, M. Gotoh, "Impact behavior of honeycomb structures with various cell specifications—numerical simulation and experiment," *International Journal of Impact Engineering*, vol. 32, no. 14, pp. 618-630, 2005.
- [17] J. R. K. McFarland, "Hexagonal cell structures under post-buckling axial load," *AIAA journal*, vol. 1, no. 6, pp. 1380-1385, 1963.
- [18] D. Q. Sun, K. Gong, G. Z. Li, "Coplanar impact dynamics of triangular honeycomb," *Journal of Shaanxi University of science and technology*, vol. 31, no. 1, pp. 98-105, 2013.
- [19] Y. Liu, X. C. Zhang, "The influence of cell micro-topology on the in-plane dynamic crushing of honeycombs," *International Journal of Impact Engineering*, vol. 36, no. 1, pp. 98-109, 2009.
- [20] X. R. Liu, "Study on coplanar mechanical behavior of I-beam honeycomb," *Shaanxi University of science and technology*, 2018.
- [21] Y. W. Huang, J. H. Feng, D. Q. Sun, "Simulation analysis of coplanar mechanical properties of square metal honeycomb materials," *Packaging Engineering*, vol. 30, no. 4, pp. 18-20+36, 2009.
- [22] J. Yu, X. J. Li, "Finite element analysis of impact properties of circular metal honeycomb core," *Packaging Engineering*, vol. 11, pp. 30-32, 2008.
- [23] Y. Fan, "Deformation mode and energy absorption of honeycomb materials under in-plane impact," *Zhejiang University*, 2008.
- [24] X. F. Huang, "Energy absorption characteristics of hierarchical honeycomb and its application," *Hunan University*, 2019.
- [25] R. Xin, X. Y. Zhang, Y. M. Xie, "Research progress of negative Poisson's ratio materials and structures," *Chinese Journal of Theoretical and Applied Mechanics*, vol. 2019, no. 3, pp. 32, 2019.
- [26] D. S. Grummon, J. A. Shaw, J. Foltz, "Fabrication of cellular shape memory alloy materials by reactive eutectic brazing using niobium," *Materials Science and Engineering: A*, vol. 438, pp. 1113-1118, 2006.
- [27] J. A. Shaw, D. S. Grummon, J. Foltz, "Superelastic NiTi honeycombs: fabrication and experiments," *Smart Materials and Structures*, vol. 16, no. 1, pp. S170, 2007.
- [28] Z. Ke, H. J. Zhang, Z. P. Tang, "Experimental study of thin-walled TiNi tubes under radial quasi-static compression," *Journal of intelligent material systems and structures*, vol. 22, no. 18, pp. 2113-2126, 2011.
- [29] S. N. Nasser, J. Y. Choi, J. B. Isaacs, "Quasi-static and dynamic buckling of thin cylindrical shape-memory shells," *Journal of Applied Mechanics*, vol. 73, no. 5, pp. 825-833, 2006.
- [30] X. Guo, X. Dong, Z. Yu, "Study on the Mechanical Properties of Bionic Protection and Self-Recovery Structures," *Materials*, vol. 13, no. 2, pp. 389, 2020.
- [31] A. Mohan, S. M. Srinivasan, M. Joshi, "Exploitation of Large Recoverable Deformations Using Weaved Shape Memory Alloy Wire-Based Sandwich Panel Configurations," *Journal of Engineering Materials and Technology*, vol. 139, no. 2, pp. 021014, 2017.